ACS Electrochemistry

pubs.acs.org/electrochem
Article

Microalgae-Based Hybrid Biophotoelectrode for Efficient Light Energy Conversion

Caio C. G. Silva, Guilherme Martins, André Luís, Hernán D. Rojas-Mantilla, Ana Rovisco, Rodrigo Martins, Elvira Fortunato, Inês A. C. Pereira, Maria V. B. Zanoni, Saulo S. Garrido, and Felipe Conzuelo*

Cite This: ACS Electrochem. 2025, 1, 1184–1193

ABSTRACT: Photosynthetic microorganisms are promising candidates for sustainable energy production in photobioelectrochemical systems. However, integrating them with electrodes is challenging due to the compartmentalized nature of photosynthetic organelles. Microalgae, in particular, have a more complex cell structure than cyanobacteria, leading to low electron transfer rates and compromising electrochemical communication. In this study, we propose a hybrid biophotoelectrode that integrates intact microalgae cells with a WO_3 semiconductor electrode using polydopamine for cell entrapment and charge transfer enhancement. The biophotoelectrode delivers photocurrents of up to 24 μA cm^{-2} under visible light illumination with an incident light power below 6.0 mW cm^{-2}. The photoelectrode performance and the origin of electron flow are investigated, confirming a substantial contribution of immobilized microalgae to the overall photocurrent. We present a proof-of-concept application of the microalgae-based hybrid electrode in combination with a formate dehydrogenase biocathode for the implementation of a biophotoelectrochemical cell for the conversion of CO_2 to formate assisted by light. The system demonstrates the potential for coupling photosynthetic processes with bioelectrochemical conversion, achieving efficient and sustainable production of value-added chemicals. These findings advance our understanding of photosynthetic cell−electrode interactions in hybrid systems, offering insights for developing photobioelectrochemical devices and innovative conversion strategies for waste products.

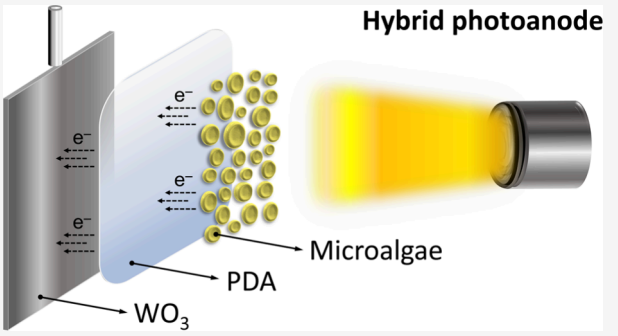

KEYWORDS: *microalgae, polydopamine, CO_2 reduction, hybrid catalysts, biophotoelectrochemical devices*

INTRODUCTION

The undeniable progress in social and industrial development has undoubtedly delivered numerous benefits in our rapidly expanding world. Yet, amidst the improved quality of life witnessed over centuries, the repercussions of these advancements are becoming more evident. Issues like energy crises and environmental pollution are visible outcomes of this progress, and the extensive use of non-renewable energy sources such as coal, oil and natural gas, which are significant contributors to environmental pollution and the emission of greenhouse gases, mainly CO_2.[1] The urgency of addressing climate change is apparent, with atmospheric CO_2 levels reaching 426.1 ppm in June 2024 and projections indicating an expected rise.[2,3] To mitigate these impacts, the scientific community is growing consensus on the need for efficient strategies to capture, store, and convert CO_2 into valuable products. In this context, photosynthesis is a vital and intricate natural process adept at transforming solar energy into chemical energy with remarkable efficiency. Its successful integration into photobioelectrochemical (PBE) devices has paved the way for diverse technological advancements.[4] These applications span from generating bioelectricity, crafting biosensors for water quality monitoring, and conducting bioelectrosynthesis to produce valuable compounds.[5,6] PBE devices utilize photosynthetic components like isolated photosystems,[7,8] thylakoid membranes,[9,10] chloroplasts,[11,12] or entire organisms such as cyanobacteria,[13,14] purple bacteria,[5] and microalgae,[15] integrated with electrodes. The biological components are abundant and offer safety, affordability, easy recyclability, and a relatively simple preparation. There is an increased interest in employing whole organisms, especially microalgae, to assemble PBE devices. Microalgae, due to their complete photosynthetic structure, self-repair mechanisms against light-induced damage, natural pathways to mitigate reactive oxygen species from

Received: February 4, 2025
Revised: April 14, 2025
Accepted: April 24, 2025
Published: May 21, 2025

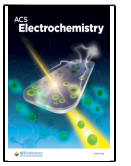

photosynthesis, and capabilities for self-replication, constitute a compelling choice for PBE approaches.[16]

Chlorella is a genus of unicellular green microalgae, with species ranging in size from 3.0 μm to 8.0 μm and with different morphology. This microorganism is known not only for its applications in the pharmaceutical and nutraceutical industries but also for its high photosynthetic capability due to the abundance of photosynthetic pigments that help in capturing light, serving in the production of renewable energy in the fabrication of biophotovoltaic cells or as feedstock for biofuel cells.[17] These microalgae can be considered a potential photosynthetic entity to be integrated into PBE systems and are the research target of this work.

It is essential to highlight that one of the significant difficulties in building a photobiohybrid platform based on whole organisms, such as microalgae, is to ensure that immobilization leads to an efficient electron transfer (ET) between the biological entity and the electrode surface.[6] Due to the complex morphology of these organisms, intricate systems of external and internal lipid membranes, and photosynthetic reactions occurring within the chloroplasts, ET becomes limited after integration with electrodes.[5,17] Achieving direct electron transfer (DET) continues to be challenging for microalgae and most photosynthetic microorganisms.[18] Therefore, the main focus of the scientific community has been the search for efficient alternatives to anchor intact organisms and guarantee a mediated electron transfer (MET) between the biological component and the electrode using electronic mediators and electrode surfaces that potentiate ET. These mediators can be broadly classified into two categories:[19] (i) exogenous diffusible mediators and (ii) polymeric-based mediators. Exogenous redox mediators are highly effective in electronic communication, ensuring electron transfer with complex biological entities even across cellular membranes.[20] However, freely diffusing redox mediators can compromise the generated photocurrent due to the poisoning effect of the photosynthetic chain and the possible occurrence of short-circuiting pathways.[21] Moreover, improper disposal of such compounds could also cause extensive environmental damage. As a result, this may not be a viable choice for the long-term operation of PBE devices. MET that uses polymer matrices has already been reported, using, for example, redox polymers based on osmium[14,15,22,23] or quinone groups[24] in combination with photosynthetic organisms, as they compete with natural electron transporters in microorganisms for enabling photoinduced electron extraction. Conductive polymers, such as polydopamine (PDA), have also been used satisfactorily as electron mediators for immobilization and electrical wiring of photosynthetic entities, including chloroplasts[11] and intact bacterial cells.[25] PDA-based conductive polymers integrate functional groups (quinones and semiquinones) that contribute to an efficient ET between the biological material and the electrode. In addition, PDA offers other favorable attributes such as solid adhesion to electrode surfaces, low toxicity, photoexcitation by light absorption in the visible region, and straightforward synthesis.

Another crucial factor for constructing PBE devices is the material used as electrode substrate in biohybrid platforms. Some substrates reported in the literature include transparent oxide semiconductors, such as fluorine-doped tin oxide (FTO)[26] and glass sheets coated with indium-doped tin oxide (ITO),[27] as well as reduced graphene oxide,[28] and gold electrodes.[15] Tungsten trioxide (WO_3), an n-type semiconductor, has been reported as an alternative material to improve photoexcitation under visible light.[29] In addition to being widely applied in photocatalytic and photoelectrocatalytic processes due to its low band-gap energy (2.5−2.8 eV), this material has been used in combination with biomolecules due to its low cost, ease of synthesis, eco-compatibility, chemical stability, and biocompatibility.[30]

This study presents the implementation and characterization of a hybrid biophotoelectrode by integrating *Chlorella* sp. cells with a WO_3 electrode modified with PDA as a conductive polymer. The resulting system offers a promising strategy for developing photohybrid electrodes with enhanced energy conversion performance. The approach significantly increases the generation of photocurrents, taking advantage of the photosynthetic nature of *Chlorella* cells, the conductivity of PDA, and the semiconductor nature of WO_3. The synergism between the described components is shown to advance the efficiency of sustainable solar energy conversion. Furthermore, as a proof-of-concept application, the microalgae-based photoanode developed is used in combination with a formate dehydrogenase biocathode for the assembly of a biophotoelectrochemical cell enabling light-assisted CO_2 conversion and the synthesis of formate.

MATERIALS AND METHODS

Algae Strain and Culture Conditions. The green microalga *Chlorella minutissima* was acquired from the Culture Collection of Autotrophic Organisms (CCALA), Institute of Botany, Třeboň, Czech Republic. Cultures were grown in 80 mL of Bold's basal medium (BBM) in 125 mL corning polycarbonate Erlenmeyer flasks at (23 ± 2) °C, with orbital shaking at 160 rpm, and illuminated by a visible LED (Vis-LED) system, using illumination periods of 12 h light:12 h dark.

Microalgae-Based Biophotoelectrode Fabrication. The WO_3 electrode was synthesized and modified with a PDA film as previously described.[11] Briefly, 1.0 cm^2 tungsten foils of 0.025 cm thickness (Sigma-Aldrich) were polished with sandpaper of different grain sizes (400, 800, 1000, and 2000), followed by cleaning in an ultrasonic bath in acetone, ethanol, and distilled water for 5 min each. Then, anodization was performed by applying 40.0 V for 15 min in a 0.7% (w/v) NH_4F solution with 0.1 M Na_2SO_4. The electrode was calcined at 450 °C for 2 h. For the deposition of the PDA film, the WO_3 substrate was immersed in a solution containing 5.0 mg mL^{-1} of dopamine in 10.0 mM Tris-HCl pH 8.5 under stirring for 4 h at 4 °C. Afterwards, the electrode was rinsed with distilled water to remove excess dopamine and PDA that was not adsorbed on the surface. The electrode was then dried with N_2. For modification with *Chlorella* cells, when the culture reached an exponential phase after 72 h of growth, the microalgae cells were collected by centrifugation at 4000 rpm for 15 min at 4 °C, yielding a final concentration of 3.0×10^6 cells mL^{-1}. The cell concentration was determined by the Fuchs-Rosenthal cell counting method. Then, 25.0 μL of the concentrated microalgae solution were deposited by drop-casting onto the PDA-WO_3 electrode and allowed to dry at room temperature. After drying, the microalgae-modified electrode was ready for measurements.

Photoelectrochemical Setup. All electrochemical measurements were performed in 0.1 M phosphate buffer solution (PBS) pH 7.0 as electrolyte, using an electrochemical cell with

https://doi.org/10.1021/acselectrochem.5c00053
ACS Electrochem. 2025, 1, 1184−1193

two compartments separated by a Nafion membrane (N-115, 0.125 mm thick, Alfa Aesar). On one side, integrating a quartz window for allowing illumination, the microalgae-based biophotoelectrode prepared as described above was inserted and used as the working electrode. An Ag/AgCl/3.0 M KCl electrode was placed in the same compartment and used as the reference electrode. A platinum wire (3.5 cm), used as an auxiliary electrode, was placed in the secondary cell compartment, thus ensuring that any reaction occurring at the counter electrode does not interfere with the performance of the biophotoelectrode. Electrochemical measurements were performed using a Biologic potentiostat/galvanostat (SP-200, Bio-Logic Science Instruments). A homemade low-power Vis-LED system (power density 5.7 mW cm^{-2}) and an LED revolver (Instytut Fotonowy) equipped with LEDs of different wavelengths and different power densities (453 nm, 3.1 mW cm^{-2}; 525 nm, 1.9 mW cm^{-2}; 590 nm, 1.8 mW cm^{-2}; and 623 nm, 3.7 mW cm^{-2}) were used as light sources for the photoelectrochemical measurements.

Photoelectrode Characterizations. The biophotoanode performance was investigated by chronoamperometry under chopped-light illumination. The photocurrent response generated by the hybrid photoelectrode was determined by calculating the difference between current responses at the end of the illumination period and those recorded under dark, considering the geometrical electrode area (1.0 cm^2). Electrochemical impedance spectroscopy (EIS) was recorded using a 5 mV potential amplitude, with measurements in the frequency range from 1.0×10^5 Hz to 0.01 Hz, 10 points per decade. Mott-Schottky analyses were obtained after recording impedance spectra at different applied potentials (between -0.6 and 1.0 V). Fluorescence confocal laser scanning microscopy images were obtained for the electrode after different fabrication steps to get information about the microalgae-based biophotoelectrode interface. A fluorescence-confocal laser scanning microscope (Zeiss LSM 880 with Fast Airyscan) was used, with a 40× oil immersion objective lens and a laser line of 561 nm. Characterizations by scanning electron microscopy (SEM) were done using a Hitachi Regulus 8220 field-emission scanning electron microscope. In previous research, comprehensive analyses were conducted to unveil the morphological and structural intricacies of the substrate. These investigations employed, X-ray diffraction, and diffuse reflectance spectroscopy, elucidating the specific characteristics and distinct properties, as summarized in Ref.[11] Photoluminescence spectra were obtained using a Horiba Jobin Yvon Fluorolog-3 FL3-122 spectrofluorometer. The measurements were performed at room temperature using a 450 W Xe-lamp; emission spectra were measured at an excitation wavelength of 315 nm. The incident photon to current conversion efficiency (IPCE) was calculated at a wavelength of 453 nm, according to the following equation:

$$\mathrm{IPCE}(\%)_{453nm} = j\left(\frac{hc/e}{P\lambda}\right) \times 100 \quad (1)$$

where j is the photocurrent density (μA cm^{-2}), P is the light power of the illumination source, λ is the light wavelength (453 nm), h is the Planck constant, c is the speed of light, and e is the elementary charge.

Biophotoelectrochemical Cell for Light-Assisted CO_2 Conversion. FdhAB was purified with an affinity chromatography in a Strep-Tactin gravity flow affinity column (IBA Lifesciences) equilibrated with binding buffer (100 mM Tris, 10 mM $NaNO_3$, 150 mM NaCl and 10% (v/v) glycerol at pH 8.0). The soluble fraction was loaded in the column and washed five times with binding buffer. The flow-through fraction was collected. Elution buffer (100 mM Tris, 10 mM $NaNO_3$, 150 mM NaCl, 10% (v/v) glycerol, 50 μM D-(+)-biotin, pH 8.0) was then added to the column. The first two elutions were collected separately from the next six elutions. After column treatment, the flow-through solution was concentrated and loaded into the column following the same protocol. After affinity purification the sample buffer was exchanged to 20 mM Tris, 10 mM $NaNO_3$, 10% (v/v) glycerol, pH 7.6 buffer and stored at -80 °C under anaerobic conditions. The quality of the purification was assessed by running sodium dodecyl-sulfate polyacrylamide gel electrophoresis (SDS-PAGE). An ITO-coated glass slide (100 nm ITO thickness, 14 − 16 Ω $\square^{-1}$; Ossila) was used as an electrode for Fdh immobilization. The electrode was first cleaned in an ultrasonic bath using acetone, ethanol, and water for 5 min each. Following this, 4.0 μL of a 20 μM Fdh solution were dropped onto the electrode surface (0.5 cm^2) and allowed to dry. The modified electrodes were characterized by cyclic voltammetry in a 0.1 M PBS solution, pH 7.0, containing 0.5 mM methyl viologen as soluble redox mediator. Before measurement, the electrolyte solution was bubbled with argon for 20 min to remove O_2. After the initial characterizations in the absence of enzyme substrate, 100 mM sodium bicarbonate was added, and the cell was bubbled with CO_2. A double chamber cell was used for coupling the microalgae-based biophotoanode and the Fdh-biocathode, using a Nafion membrane (N-115, 0.125 mm thick, Alfa Aesar) to separate the two electrode compartments, each of them with 10.0 mL of electrolyte solution. The polarization curve was obtained by recording the current flow under illumination and in the presence of CO_2 at different applied cell voltages using a Biologic potentiostat/galvanostat (SP-200, Bio-Logic Science Instruments) operated with the EC-Lab software. Formate quantification was performed using an enzymatic assay with commercially available formate dehydrogenase from *Candida boidinii* (Sigma-Aldrich). The enzyme was added to a 100 μM NAD^+ solution (buffered with 57 mM sodium phosphate, pH 7.0) at a final concentration of 0.02 U mL^{-1}. An aliquot of 50 μL sample was mixed with 150 μL of the Fdh-NAD^+ solution in a 96-well plate and incubated at 37 °C for 180 min. Absorbance at 340 nm was then measured to detect NADH produced, using an extinction coefficient ($\varepsilon_{340\ nm}$) of 6.22 mM^{-1} cm^{-1}. Since the reaction has a 1:1 stoichiometry, the amount of NADH produced is directly related to the formate concentration in the sample.

RESULTS AND DISCUSSION

Performance of Microalgae-Based Hybrid Photoanodes. The photocurrent responses associated with the integration of the different components of the hybrid biophotoelectrode were first investigated. As illustrated in Figure 1A, the photocurrent generated by the WO_3 substrate alone (a) had a minor contribution of about 5.0 μA cm^{-2} under Vis-LED illumination (see Emission spectrum in Figure S1). When modifying the WO_3 substrate with microalgae (Figure 1A,b), the photocurrent signal did not experience a significant increase, implying that DET between the microalgae and the inorganic semiconductor material is rather limited due to the complex cell membrane structure of the photosynthetic microorganism. As a strategy to improve ET, the WO_3

https://doi.org/10.1021/acselectrochem.5c00053
ACS Electrochem. 2025, 1, 1184−1193

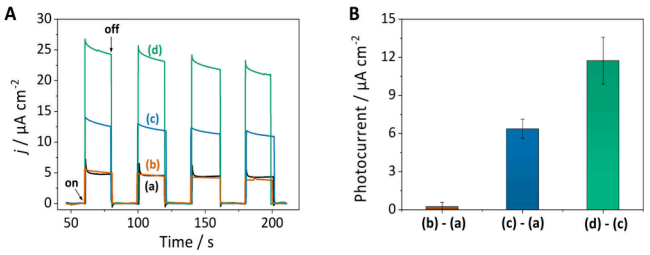

Figure 1. (A) Current density responses under chopped-light illumination for WO_3 (a), microalgae-WO_3 (b), PDA-WO_3 (c), and microalgae-PDA-WO_3 (d). Responses at an applied potential of 0.5 V (vs. Ag/AgCl/3.0 M KCl). PBS 0.1 M, pH 7.0. Vis-LED, 20 s on/off cycles. (B) Comparative analysis of the photocurrent responses, showing the contribution after the distinct stages of biophotoelectrode construction, difference in responses as indicated in panel (A). Error bars represent the standard deviation (n = 3 different photoelectrodes).

electrode was modified with a PDA film for the subsequent immobilization of microalgae under MET with the electrode surface. The photocurrent responses indicated a prominent increase after each modification step. After the integration of the PDA film, the increase in photocurrent (Figure 1A,c) was expected as a result of PDA light absorption in the visible region of the electromagnetic spectrum, which promotes charge separation in combination with the semiconductor electrode (Figure S2A).[31,32] This has been confirmed by a Mott-Schottky analysis (Figure S3) revealing substantial changes in the flat-band potential (E_{fb}), leading to a lowering in E_{fb} after PDA modification as a result of the PDA film as an effective photosensitizer for the absorption of visible light, as also confirmed by photoluminescence spectra (Figure S2B).[32−34] After additional modification with microalgae, a substantial increase in photocurrent was observed (Figure 1A,d), confirming the possibility for extraction of electrons from the photosynthetic cells, in agreement with previous reports.[35−37] PDA promotes ET through the presence of redox-active groups involving catechol/quinone pairs in the polymer structure, which was also confirmed by control experiments replacing the semiconductor substrate (see Figure S4). Moreover, PDA provides a biocompatible matrix for the strong adhesion of biological material ensuring the immobilization of microalgae onto the electrode.[11,38,39] A comparative analysis of the photocurrents obtained after the distinct stages of photoelectrode construction is presented in Figure 1B showing the different contributions to the overall response after each modification step. The results obtained highlight a notable performance in photocurrent generation with the hybrid assembly.

Electrochemical Characterizations. The microalgae-based biophotoelectrode was investigated by means of electrochemical impedance spectroscopy to characterize and understand the electronic communication after integrating the different components used to modify the WO_3 electrode. Figure S5 shows Nyquist plots obtained for the EIS characterizations under dark and light conditions using $[Fe(CN)_6]^{3-}/[Fe(CN)_6]^{4-}$ as a redox probe. From the data obtained, the charge transfer resistance (R_{ct}) was calculated and used to estimate the corresponding kinetic rates for electron transfer (k^0),[40] as summarized in Table S1. The results revealed a larger impedance for the unmodified WO_3 substrate in the dark compared with the experiment performed under illumination, in line with the expectations for a semiconductor material. After modification with PDA, the charge transfer resistance decreased significantly. This result underscores the impact of PDA, promoting electronic communication and favoring charge separation when the photoelectrode is illuminated. After modification of the electrode surface with microalgae cells, an increase in charge transfer resistance was observed due to a partial blocking of the electrode surface by the immobilized cells, leading to an increase in resistance for the transfer of electrons between the redox probe and the electrode surface. This confirmed the additional function of PDA as a suitable support for the entrapment of cells over the electrode surface, enabling microalgae immobilization.

The hybrid nature of the biophotoelectrode requires finding the optimal conditions for maximum photocurrent generation supported by the contribution of the different components under light excitation. The applied potential significantly influences the electron transfer from the different light-sensitive sources, which is essential for photocurrent generation with the biological and semiconductor components. Figure 2 demonstrates the impact of the applied potential on

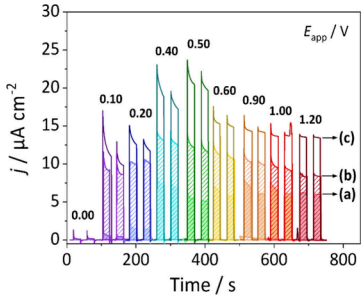

Figure 2. Effect of applied potential on the photocurrent response obtained for WO_3 (a), PDA-WO_3 (b), and microalgae-PDA-WO_3 (c). Applied potentials (E_{app}) vs. Ag/AgCl/3.0 M KCl as indicated in the graph. PBS 0.1 M, pH 7.0; Vis-LED, 20 s on/off cycles.

photocurrent generation with WO_3 (a), PDA-WO_3 (b), and microalgae-PDA-WO_3 (c) electrodes. For the WO_3 electrode, increasing the applied potential resulted in a gradual increase in photocurrent for $E_{app} \geq 400$ mV (vs. Ag/AgCl/3.0 M KCl). However, the WO_3 electrode alone exhibited only a limited photocurrent response compared to the modified electrodes. The modification with PDA proved crucial for enhancing electron transfer. Thus, even without microalgae, the PDA-WO_3 electrode displayed a superior photoelectrochemical response already at E_{app} = 100 mV (vs. Ag/AgCl/3.0 M KCl). For the complete hybrid electrode (microalgae-PDA-WO_3) the highest response was attained at an applied potential of 500 mV (vs. Ag/AgCl/3.0 M KCl). This value was selected for subsequent measurements and characterizations.

Hybrid Photoelectrode Optimizations. To achieve the optimal biophotoelectrode composition, the thickness of the PDA layer was first investigated. For this, electrodes were prepared using different PDA deposition times and the photocurrent responses were compared in the presence and absence of microalgae. As summarized in Figure S6, only small variations in photocurrent output were observed for electrodes without microalgae modification. In contrast, electrodes in the presence of microalgae exhibited a clear optimum when PDA deposition was performed for 4 h. The observed superior

https://doi.org/10.1021/acselectrochem.5c00053
ACS Electrochem. 2025, 1, 1184−1193

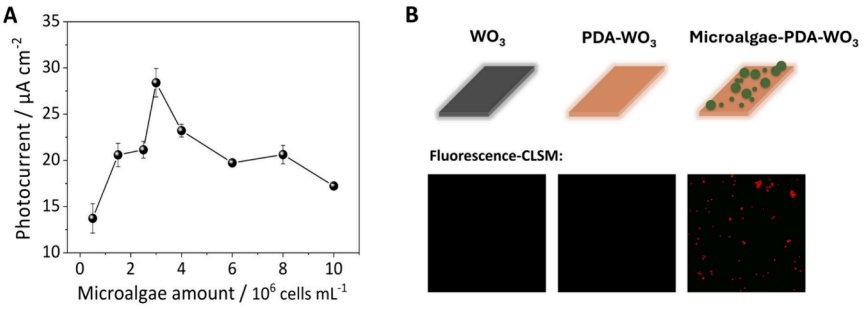

Figure 3. (A) Photocurrent response for different amounts of microalgae used in the fabrication of the hybrid biophotoelectrode. Error bars represent the standard deviation (n = 3 different electrodes). (B) Characterization of WO_3, PDA-WO_3, and microalgae-PDA-WO_3 electrodes by fluorescence confocal laser scanning microscopy (CLSM).

response could be attributed to an ideal film thickness ensuring adequate immobilization of cells and an efficient ET. This was supported by previous observations indicating similar optimal conditions.[11] In addition, the amount of microalgae used for electrode fabrication was optimized. As shown in Figure 3A, solutions of variable microalgae concentration in the range of (0.5 to 10.0)×10^6 cells mL^{-1} were investigated for this purpose. An increase in photocurrent was observed with an increasing amount of cells, reaching a maximum photocurrent response when a concentration of 3.0×10^6 cells mL^{-1} was used for electrode modification. This amount was selected as the optimum for biophotoelectrode fabrication. For higher concentrations, a decreasing trend in photocurrent response was observed, most likely due to a blocking of the electrode surface at high cell loadings, preventing a sufficient and homogeneous arrival of light to other immobilized cells and the underlying semiconductor/PDA material, consequently leading to a decrease in photocurrent. To further investigate the hybrid photoelectrode, the optimal assembly was characterized by confocal fluorescence microscopy (Figure 3B). No fluorescence response was observed for WO_3 only and PDA-modified WO_3, as these materials do not present autofluorescence under the excitation conditions used.[11,41] In contrast, the image obtained for the microalgae-PDA-WO_3 electrode confirmed the presence of bright red spots spread across the electrode surface, which originated from the autofluorescence of chlorophyll in microalgae and confirmed the immobilization of *Chlorella* cells over the electrode. Scanning electron microscopy characterization was also performed (Figure S7). These images revealed the characteristic nanoporous structure of WO_3,[42,43] without substantial structural changes after modification with PDA. For the complete hybrid electrode, the presence of microalgae was evident, showing photosynthetic cells spread over the electrode surface, which contribute to the photocurrent response while allowing light reaching the electrode surface underneath for the overall production of photocurrent with the hybrid biophotoelectrode.

Response under Different Illumination Conditions. The performance of the biophotoelectrode in terms of photocurrent response was evaluated at a constant applied potential of 500 mV (vs. Ag/AgCl/3.0 M KCl) using different illumination intensities, ranging from 0.4 mW cm^{-2} to a maximum of 5.7 mW cm^{-2} provided by a Vis-LED illumination system. The results obtained (Figure 4A), exhibited a continuous increase in photocurrent response with increasing illumination intensity until a maximum of 28.2 μA cm^{-2} for 100% light power. The responses observed demonstrate the

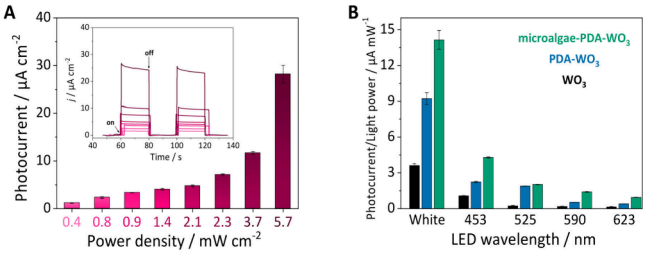

Figure 4. (A) Impact of white-light LED illumination intensity on the photocurrent response for the microalgae-PDA-WO_3 biophotoelectrode. Inset: exemplary amperometric traces under chopped-light illumination for the different light intensities. Applied potential: 0.5 V (vs. Ag/AgCl/3.0 M KCl). PBS 0.1 M, pH 7.0; 20 s light on/off cycles. (B) Effect of illumination wavelength on the photocurrent response for the different steps of biophotoelectrode construction. The photocurrent response is normalized by the light power under each light condition. Error bars represent the standard deviation (n = 3 different electrodes).

capability of the hybrid biophotoelectrode to generate remarkable photocurrents even when using a low-power LED illumination system that delivers a maximum power below 6 mW cm^{-2}. The performance of the biophotoelectrode is significant, considering that the biological component contributing to photocurrent generation is a microalgae, a photosynthetic organism with a more complex cellular structure than conventionally used bacterial counterparts, such as cyanobacteria, in PBE devices.[44] A comparison of performance for different biophotoelectrodes based on the use of oxygenic photosynthetic microorganisms is presented in Table S2. The photoelectrode developed is clearly superior to other microalgae-based photoelectrodes and even several cyanobacteria-based photoelectrodes, even when considering only the contribution of the photosynthetic cells to the overall photoelectrochemical response (see Figure 1). Moreover, since different components contribute to the total photocurrent generated as a result of the hybrid nature of the photoelectrode, the performance obtained is remarkable.

Origin of Electron Flow. The biophotoelectrode performance was investigated using monochromatic illumination of different wavelengths within the visible range of the electromagnetic spectrum. Figure 4B summarizes the photocurrent response obtained for WO_3 only, WO_3 modified with PDA, and the complete microalgae-PDA-WO_3 biophotoelectrode under different illumination conditions. The responses have been normalized by the intensity of the diverse illumination wavelengths and are also compared with the photocurrent obtained using white light illumination (see Figure S1). The

https://doi.org/10.1021/acselectrochem.5c00053
ACS Electrochem. 2025, 1, 1184−1193

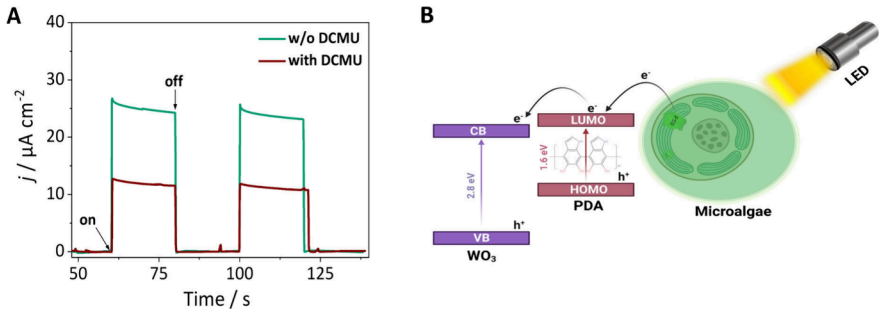

Figure 5. (A) Effect of the addition of DCMU to the photocurrent generated by the microalgae-based hybrid biophotoelectrode. Applied potential: 0.5 V (vs. Ag/AgCl/3.0 M KCl). PBS 0.1 M, pH 7.0; 20 s light on/off cycles. (B) Schematic of electron transfer at the microalgae-based biophotoanode. The photosynthetic microorganisms oxidize H_2O and transfer some of the resulting energized electrons to the electrode. An extracellular electron transfer pathway is shown, mediated by PDA.

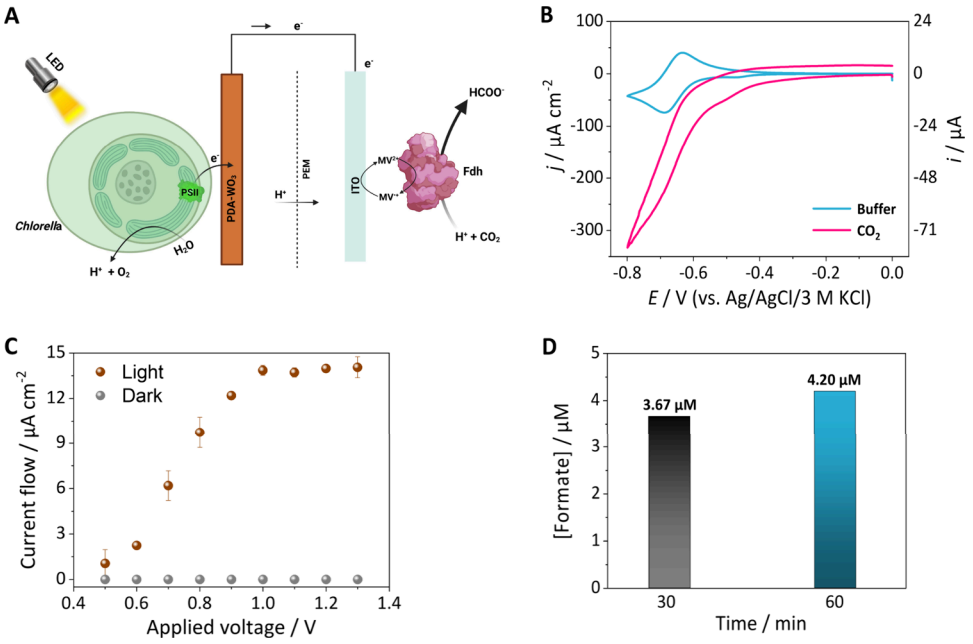

Figure 6. (A) Biophotoelectrochemical cell constituted by the microalgae-based hybrid electrode as photoanode and an Fdh-modified electrode as biocathode. The assembly allows CO_2 reduction to formate assisted by light. ITO: indium-doped tin oxide electrode. MV: methyl viologen. PEM: proton exchange membrane. (B) Voltammetric characterization of the Fdh-biocathode in the absence (blue curve) and presence (pink curve) of CO_2 in solution (third cycle, see Figure S9). Electrolyte: 0.1 M PBS, pH 7.0 with 0.5 mM MV as redox mediator in solution. Scan rate: 10 mV s^{-1}. (C) Polarization curve obtained in the characterization of the biophotoelectrochemical cell. Photoanode under light or dark conditions (as indicated) and biocathode in the presence of CO_2. Error bars represent the standard deviation (n = 3 different electrodes). (D) Formate quantification after 30 and 60 min of BPV operation. E_{app} = 1.0 V.

results revealed the contributions of the different components constituting the hybrid biophotoelectrode. For WO_3, photocurrent generation was evident at 453 nm, while only a minor contribution was obtained at higher wavelengths, in line with the bandgap of the semiconductor material, presenting minimum light absorption for wavelengths higher than 500 nm.[45,46] The responses for PDA-modified WO_3 underlined the capability of the polymer to absorb visible light and contribute to photocurrent generation. The integration of microalgae made it possible to further increase the photocurrent response due to the photosynthetic nature of the microbial cells, absorbing light in the visible region. The peculiar behavior observed at 525 nm, resulting in a negligible increase in photocurrent after the integration of microalgae, aligns with the absorption spectrum of the microbial cells in solution (Figure S8), presenting a minimum absorption within this spectral region. As expected, the use of white light increased the response for all components due to the higher number of illumination wavelengths contributing to photocurrent generation. The quantum efficiency of the photoelectrode was evaluated as the incident photon to current conversion efficiency (IPCE), calculated at a wavelength of 453 nm. The calculated efficiencies were 1.0% for WO_3 only, 2.1% for PDA-WO_3, and 4.2% for the microalgae-modified photoelectrode. The IPCE results are consistent with the photocurrent responses shown previously, where the maximum was obtained for microalgae-PDA-WO_3 electrodes.

Since the immobilized microalgae have a significant contribution to the photocurrent generated (Figure 1 and Figure 4B), the source of electrons from the photosynthetic electron transport chain was also investigated. For this, the performance of biophotoelectrodes was compared before and after incubation with 3-(3,4-dichlorophenyl)-1,1-dimethylurea (DCMU), a known photosynthetic inhibitor that prevents the

https://doi.org/10.1021/acselectrochem.5c00053
ACS Electrochem. 2025, 1, 1184−1193

flow of electrons exiting photosystem II (PSII) to reach further steps in the photosynthetic chain. The presence of DCMU caused a drastic decrease in photocurrent, reaching similar values as those observed for photoelectrodes in the absence of microalgae (Figure 5A). Therefore, it could be concluded that electrons are extracted from PSII after performing water oxidation and contribute to the overall photocurrent response obtained with the hybrid electrode (Figure 5B).

Biophotoelectrochemical Cell for Light-Assisted CO_2 Conversion. As a proof-of-concept application of the developed biophotoelectrode, a biophotoelectrochemical cell was assembled constituted by the microalgae-based hybrid photoanode coupled to a formate dehydrogenase (Fdh) biocathode. Fdh-modified electrodes have proven to be a promising strategy for the biocatalytic conversion of CO_2.[47−50] The aim of this assembly was to demonstrate the possibility of using the electrons generated by the photoanode to assist the enzymatic conversion of CO_2 into formate (see Figure 6A). The biocathode consisted of an indium-doped tin oxide (ITO) electrode on which FdhAB from *Desulfovibrio vulgaris* Hildenborough[51] was adsorbed and made use of methyl viologen (MV) as redox mediator in solution. The bioelectrode was characterized by cyclic voltammetry (Figure 6B). In the absence of CO_2, the characteristic response for the $MV^{2+}/MV^{\bullet+}$ redox couple was observed (Figure 6B, blue curve). When introducing CO_2, a significant increase in cathodic current was obtained (Figure 6B, pink curve), reflecting the enzyme-catalyzed CO_2 reduction reaction mediated by MV for the transfer of electrons between the ITO electrode and the immobilized enzyme. After coupling the two electrodes in the biophotoelectrochemical cell, the polarization curve for the assembly was investigated (Figure 6C). No current flow was observed under dark conditions as the photoanode is unable to deliver electrons. Under illumination, a significant current flow was observed already at an applied voltage of 600 mV, as expected from the photoanode characterization presented in Figure 2 and the increase in catalytic current with the biocathode at potentials more negative than -500 mV vs. Ag/AgCl/3 M KCl (Figure 6B). A maximum current output of 14 μA cm^{-2} was obtained at voltages above 1.0 V. The biophotoelectrochemical cell was also investigated in terms of formate production under constant illumination conditions, being able to produce up to 42 nmol of formate after 60 min of continuous operation (Figure 6D). Note that under dark and in the absence of current flow no formate production was detected. The production of formate over time under illumination confirmed the sustained electrocatalytic activity of the assembly at least for the first 30 min, with a calculated Faradaic efficiency of 86%. The production rate was observed to decrease at longer times. This could be explained by the rather limited stability of the hybrid photoanode, as shown in Figure S10 for the evaluation of long-term photocurrent generation. Although the photoelectrode requires further investigations aiming on an improved stability, the results highlight the feasibility of using the biophotoelectrochemical system for carbon dioxide fixation, effectively combining the light-harvesting capabilities of the hybrid photoelectrode with the specific catalytic activity of Fdh.

CONCLUSIONS

In this study, we implemented a hybrid system for photocurrent generation based on a semiconductor substrate modified with intact microalgae. To construct the biophotoelectrode, *Chlorella* sp. cells were immobilized on the surface of nanoporous WO_3. Experimental characterizations showed that photocurrent generation through DET between the photosynthetic cells and the electrode surface was challenging, yielding only a negligible increase in photocurrent response when compared to the bare semiconductor material as a result of the complex microalgae cellular structure compromising communication between the photosynthetic chain within the cells and the electrode. To overcome this challenge, we proposed the additional modification of the electrode substrate with PDA. This polymer exhibited advantageous properties to enhance the performance of the hybrid system, including a stable adsorption over the semiconductor electrode, a suitable matrix for the entrapment of microalgae cells, and the improvement of charge separation and electronic communication. This contributed to the generation of photocurrents as high as 28.2 μA cm^{-2}. We performed different characterizations of the biohybrid photoelectrode, including the influence of the applied potential on photocurrent generation, showing a maximum performance at 500 mV vs. Ag/AgCl/3.0 M KCl. Additionally, we investigated the influence of the light power used for photoelectrode excitation, revealing that relatively high photocurrents are already obtained even when using a low-power LED-based illumination system providing a maximum power of 5.7 mW cm^{-2}. We have also shown that the biological component, i.e., the photosynthetic microalgae cells, has a substantial contribution to the overall photocurrent generated by the hybrid system, accounting for about 50% of the total response. This is a promising result, as we show the possibility for an improved extraction of electrons from a complex microorganism, such as microalgae, interfaced with an electrode, complementing the majority of reports nowadays available in literature dealing with the use of cyanobacterial cells as biological photosynthetic components. Finally, the developed hybrid photoelectrode has been successfully applied in a biophotoelectrochemical system in combination with an enzymatic biocathode to attain a photoelectrochemical cell for light-assisted CO_2 reduction. The results presented in this work open up possibilities for applying this microalgae-based system in biophotovoltaic devices, offering an exciting alternative for developing sustainable light energy conversion systems.

ASSOCIATED CONTENT

Supporting Information

The Supporting Information is available free of charge at https://pubs.acs.org/doi/10.1021/acselectrochem.5c00053.

Emission spectrum of illumination source; absorbance and photoluminescence spectra for WO_3 and PDA-WO_3; Mott−Schottky analysis; control response with a glassy carbon electrode; impedance spectra under dark and light conditions; PDA deposition time study; SEM characterizations; UV−Vis absorption of microalgae in solution; biocathode stability; photoanode stability; calculated R_{ct} and k^0 values; and literature comparison of photosynthetic microorganism-based biophotoelectrodes (PDF)

AUTHOR INFORMATION

Corresponding Author

Felipe Conzuelo − *Instituto de Tecnologia Química e Biológica António Xavier, Universidade Nova de Lisboa,*

https://doi.org/10.1021/acselectrochem.5c00053
ACS Electrochem. 2025, 1, 1184−1193

*2780-157 Oeiras, Portugal; orcid.org/0000-0002-3316-2642; Email: felipe.conzuelo@itqb.unl.pt

Authors

Caio C. G. Silva − *Instituto de Tecnologia Química e Biológica António Xavier, Universidade Nova de Lisboa, 2780-157 Oeiras, Portugal; Instituto de Química, Universidade Estadual Paulista (UNESP), Araraquara 14800-060 São Paulo, Brazil*

Guilherme Martins − *Instituto de Tecnologia Química e Biológica António Xavier, Universidade Nova de Lisboa, 2780-157 Oeiras, Portugal*

André Luís − *Instituto de Tecnologia Química e Biológica António Xavier, Universidade Nova de Lisboa, 2780-157 Oeiras, Portugal; orcid.org/0009-0007-6903-1779*

Hernán D. Rojas-Mantilla − *Instituto de Química, Universidade Estadual Paulista (UNESP), Araraquara 14800-060 São Paulo, Brazil; orcid.org/0000-0002-9555-5046*

Ana Rovisco − *CENIMAT/i3N, Department of Materials Science, NOVA School of Science and Technology (NOVA FCT) and CEMOP/UNINOVA, NOVA University Lisbon, 2829-516 Caparica, Portugal; orcid.org/0000-0001-6240-3743*

Rodrigo Martins − *CENIMAT/i3N, Department of Materials Science, NOVA School of Science and Technology (NOVA FCT) and CEMOP/UNINOVA, NOVA University Lisbon, 2829-516 Caparica, Portugal*

Elvira Fortunato − *CENIMAT/i3N, Department of Materials Science, NOVA School of Science and Technology (NOVA FCT) and CEMOP/UNINOVA, NOVA University Lisbon, 2829-516 Caparica, Portugal*

Inês A. C. Pereira − *Instituto de Tecnologia Química e Biológica António Xavier, Universidade Nova de Lisboa, 2780-157 Oeiras, Portugal; orcid.org/0000-0003-3283-4520*

Maria V. B. Zanoni − *Instituto de Química, Universidade Estadual Paulista (UNESP), Araraquara 14800-060 São Paulo, Brazil*

Saulo S. Garrido − *Instituto de Química, Universidade Estadual Paulista (UNESP), Araraquara 14800-060 São Paulo, Brazil*

Complete contact information is available at: https://pubs.acs.org/10.1021/acselectrochem.5c00053

Notes

The authors declare no competing financial interest.

■ ACKNOWLEDGMENTS

The authors are grateful to the following Brazilian and Portuguese research funding agencies for the financial support provided during this research: Coordenação de Aperfeiçoamento de Pessoal de Nível Superior - Brazil (CAPES), Conselho Nacional de Pesquisa e Desenvolvimento (CNPq) [grant number #465571/2014-0], Fundação de Amparo à Pesquisa do Estado de São Paulo, FAPESP [grant number #2014/50945-4]; and FCT - Fundação para a Ciência e a Tecnologia, I.P., through grant [2022.07024.PTDC], MOST-MICRO-ITQB R&D Unit [UIDB/04612/2020, UIDP/04612/2020], LS4FUTURE Associated Laboratory [LA/P/0087/2020], and i3N/CENIMAT Associated Laboratory [LA/P/0037/2020, UIDP/50025/2020 and UIDB/50025/2020]. C.C.G.S. and H.D.R.M. acknowledge Pró-Reitoria de Pós-Graduação (PROPG)-Unesp [grant number #44/2022], CNPq [grant number #152114/2022-0], and FAPESP [grant number #2024/04167-1] for granting a scholarship. F.C. acknowledges CAPES for an Internationalization Scholarship [CAPES/PRINT #47/2023] and FCT for the researcher contract [2022.05842.CEECIND/CP1725/CT0001] under the Scientific Employment Stimulus − Individual Call 2022. This work was partially supported by PPBI - Portuguese Platform of BioImaging (PPBI-POCI-01-0145-FEDER-022122) co-funded by national funds from OE - "Orçamento de Estado" and by european funds from FEDER - "Fundo Europeu de Desenvolvimento Regional".

■ ABBREVIATIONS

BBM, Bold's basal medium; BPV, biophotovoltaic; DCMU, 3-(3,4-dichlorophenyl)-1,1-dimethylurea; DET, direct electron transfer; EIS, electrochemical impedance spectroscopy; ET, electron transfer; Fdh, formate dehydrogenase; FTO, fluorine-doped tin oxide; IPCE, incident photon to current conversion efficiency; ITO, indium-doped tin oxide; LED, light-emitting diode; MET, mediated electron transfer; MV, methyl viologen; PBE, photobioelectrochemical; PBS, phosphate buffer solution; PDA, polydopamine; PSII, photosystem II; SDS-PAGE, sodium dodecyl-sulfate polyacrylamide gel electrophoresis; Vis, visible; WO_3, tungsten trioxide

■ REFERENCES

(1) Ángeles Fernandez, M.; Ángeles Sanromán, M.; Marks, S.; Makinia, J.; Gonzalez del Campo, A.; Rodrigo, M.; Fernandez, F. J. A grey box model of glucose fermentation and syntrophic oxidation in microbial fuel cells. *Bioresour. Technol.* **2016**, *200*, 396−404.

(2) *Earth's CO_2 Home Page*. https://www.co2.earth/ (accessed 2024-08-27).

(3) *Climate Change: Atmospheric carbon dioxide | NOAA Climate.gov*. http://www.climate.gov/news-features/understanding-climate/climate-change-atmospheric-carbon-dioxide (accessed 2024-08-27).

(4) LaVan, D. A.; Cha, J. N. Approaches for biological and biomimetic energy conversion. *Proc. Natl. Acad. Sci. U. S. A.* **2006**, *103* (14), 5251−5255.

(5) Torquato, L. D. de M.; Grattieri, M. Photobioelectrochemistry of intact photosynthetic bacteria: Advances and future outlook. *Curr. Opin. Electrochem.* **2022**, *34*, 101018.

(6) Grattieri, M.; Beaver, K.; Gaffney, E. M.; Dong, F.; Minteer, S. D. Advancing the fundamental understanding and practical applications of photo-bioelectrocatalysis. *Chem. Commun.* **2020**, *56* (61), 8553−8568.

(7) Wang, P.; Frank, A.; Zhao, F.; Szczesny, J.; Junqueira, J. R. C.; Zacarias, S.; Ruff, A.; Nowaczyk, M. M.; Pereira, I. A. C.; Rögner, M.; Conzuelo, F.; Schuhmann, W. Closing the gap for electronic short-circuiting: Photosystem I mixed monolayers enable improved anisotropic electron flow in biophotovoltaic devices. *Angew. Chem. Int. Ed.* **2021**, *60* (4), 2000−2006.

(8) Wang, P.; Zhao, F.; Hartmann, V.; Nowaczyk, M. M.; Ruff, A.; Schuhmann, W.; Conzuelo, F. Reassessing the rationale behind herbicide biosensors: The case of a photosystem II/redox polymer-based bioelectrode. *Bioelectrochemistry* **2020**, *136*, 107597.

(9) Takeuchi, R.; Suzuki, A.; Sakai, K.; Kitazumi, Y.; Shirai, O.; Kano, K. Construction of photo-driven bioanodes using thylakoid membranes and multi-walled carbon nanotubes. *Bioelectrochemistry* **2018**, *122*, 158−163.

(10) Calkins, J. O.; Umasankar, Y.; O'Neill, H.; Ramasamy, R. P. High photo-electrochemical activity of thylakoid-carbon nanotube composites for photosynthetic energy conversion. *Energy Environ. Sci.* **2013**, *6* (6), 1891−1900.

(11) Silva, C. C. G.; Torquato, L. D. de M.; de Araújo, B. C.; Mantilla, H. D. R.; Zanoni, M. V. B.; Garrido, S. S. Assessment of

WO_3 electrode modified with intact chloroplasts as a novel biohybrid platform for photocurrent improvement. *Bioelectrochemistry* **2022**, *147*, 108177.
(12) Hasan, K.; Milton, R. D.; Grattieri, M.; Wang, T.; Stephanz, M.; Minteer, S. D. Photobioelectrocatalysis of intact chloroplasts for solar energy conversion. *ACS Catal.* **2017**, *7* (4), 2257−2265.
(13) Sekar, N.; Umasankar, Y.; Ramasamy, R. P. Photocurrent generation by immobilized cyanobacteria via direct electron transport in photo-bioelectrochemical cells. *Phys. Chem. Chem. Phys.* **2014**, *16* (17), 7862−7871.
(14) Gacitua, M.; Urrejola, C.; Carrasco, J.; Vicuña, R.; Srain, B. M.; Pantoja-Gutiérrez, S.; Leech, D.; Antiochia, R.; Tasca, F. Use of a thermophile desiccation-tolerant cyanobacterial culture and Os redox polymer for the preparation of photocurrent producing anodes. *Front. Bioeng. Biotechnol.* **2020**, *8*, 900.
(15) Herrero-Medina, Z.; Wang, P.; Lielpetere, A.; Bashammakh, A. S.; Alyoubi, A. O.; Katakis, I.; Conzuelo, F.; Schuhmann, W. A biophotoelectrode based on boronic acid-modified *Chlorella vulgaris* cells integrated within a redox polymer. *Bioelectrochemistry* **2022**, *146*, 108128.
(16) McCormick, A. J.; Bombelli, P.; Bradley, R. W.; Thorne, R.; Wenzel, T.; Howe, C. J. Biophotovoltaics: Oxygenic photosynthetic organisms in the world of bioelectrochemical systems. *Energy Environ. Sci.* **2015**, *8* (4), 1092−1109.
(17) Ru, I. T. K.; Sung, Y. Y.; Jusoh, M.; Wahid, M. E. A.; Nagappan, T. *Chlorella vulgaris*: A perspective on its potential for combining high biomass with high value bioproducts. *Appl. Phycol.* **2020**, *1* (1), 2−11.
(18) Bradley, R. W.; Bombelli, P.; Rowden, S. J. L.; Howe, C. J. Biological photovoltaics: Intra- and extra-cellular electron transport by cyanobacteria. *Biochem. Soc. Trans.* **2012**, *40* (6), 1302−1307.
(19) Weliwatte, N. S.; Grattieri, M.; Minteer, S. D. Rational design of artificial redox-mediating systems toward upgrading photo-bioelectrocatalysis. *Photochem. Photobiol. Sci.* **2021**, *20* (10), 1333−1356.
(20) Clifford, E. R.; Bradley, R. W.; Wey, L. T.; Lawrence, J. M.; Chen, X.; Howe, C. J.; Zhang, J. Z. Phenazines as model low-midpoint potential electron shuttles for photosynthetic bioelectrochemical systems. *Chem. Sci.* **2021**, *12* (9), 3328−3338.
(21) Buesen, D.; Hoefer, T.; Zhang, H.; Plumeré, N. A kinetic model for redox-active film based biophotoelectrodes. *Faraday Discuss.* **2019**, *215* (0), 39−53.
(22) Hasan, K.; Patil, S. A.; Górecki, K.; Leech, D.; Hägerhäll, C.; Gorton, L. Electrochemical communication between heterotrophically grown *Rhodobacter capsulatus* with electrodes mediated by an osmium redox polymer. *Bioelectrochemistry* **2013**, *93*, 30−36.
(23) Hasan, K.; Yildiz, H. B.; Sperling, E.; Conghaile, P. Ó.; Packer, M. A.; Leech, D.; Hägerhäll, C.; Gorton, L. Photo-electrochemical communication between cyanobacteria (*Leptolyngbia* sp.) and osmium redox polymer modified electrodes. *Phys. Chem. Chem. Phys.* **2014**, *16* (45), 24676−24680.
(24) Grattieri, M.; Patterson, S.; Copeland, J.; Klunder, K.; Minteer, S. D. Purple bacteria and 3D redox hydrogels for bioinspired photo-bioelectrocatalysis. *ChemSusChem* **2020**, *13* (1), 230−237.
(25) Torquato, L. D. de M.; Matteucci, R. M.; Stufano, P.; Vona, D.; Farinola, G. M.; Trotta, M.; Zanoni, M. V. B.; Grattieri, M. Photobioelectrocatalysis of intact photosynthetic bacteria exposed to dinitrophenol. *ChemElectroChem.* **2023**, *10* (12), No. e202300013.
(26) Thorne, R.; Hu, H.; Schneider, K.; Bombelli, P.; Fisher, A.; Peter, L. M.; Dent, A.; Cameron, P. J. Porous ceramic anode materials for photo-microbial fuel cells. *J. Mater. Chem.* **2011**, *21* (44), 18055−18060.
(27) Ng, F.-L.; Phang, S.-M.; Periasamy, V.; Yunus, K.; Fisher, A. C. Evaluation of algal biofilms on indium tin oxide (ITO) for use in biophotovoltaic platforms based on photosynthetic performance. *PLoS One* **2014**, *9* (5), No. e97643.
(28) Ng, F.-L.; Jaafar, M. M.; Phang, S.-M.; Chan, Z.; Salleh, N. A.; Azmi, S. Z.; Yunus, K.; Fisher, A. C.; Periasamy, V. Reduced graphene oxide anodes for potential application in algae biophotovoltaic platforms. *Sci. Rep.* **2014**, *4* (1), 7562.
(29) Assadullah, I.; Malik, J. H.; Shafi, A.; Tomar, R. Growth of Crystalline WO3-ZnSe Nanocomposites: An approach to optical, electrochemical, and catalytic properties. *Sci. Rep.* **2022**, *12* (1), 3962.
(30) Santos, L.; Silveira, C. M.; Elangovan, E.; Neto, J. P.; Nunes, D.; Pereira, L.; Martins, R.; Viegas, J.; Moura, J. J. G.; Todorovic, S.; Almeida, M. G.; Fortunato, E. Synthesis of WO_3 nanoparticles for biosensing applications. *Sens. Actuators B Chem.* **2016**, *223*, 186−194.
(31) Loget, G.; Yoo, J. E.; Mazare, A.; Wang, L.; Schmuki, P. Highly controlled coating of biomimetic polydopamine in TiO_2 nanotubes. *Electrochem. Commun.* **2015**, *52*, 41−44.
(32) Mao, W.-X.; Lin, X.-J.; Zhang, W.; Chi, Z.-X.; Lyu, R.-W.; Cao, A.-M.; Wan, L.-J. Core-shell structured TiO_2@polydopamine for highly active visible-light photocatalysis. *Chem. Commun.* **2016**, *52* (44), 7122−7125.
(33) Torquato, L. D. de M.; Pastrian, F. A. C.; Perini, J. A. L.; Irikura, K.; de L. Batista, A. P.; de Oliveira-Filho, A. G. S.; Córdoba de Torresi, S. I.; Zanoni, M. V. B. Relation between the nature of the surface facets and the reactivity of Cu_2O nanostructures anchored on TiO_2NT@PDA electrodes in the photoelectrocatalytic conversion of CO_2 to methanol. *Appl. Catal. B Environ.* **2020**, *261*, 118221.
(34) Bailey, C. G.; Nothling, M. D.; Fillbrook, L. L.; Vo, Y.; Beves, J. E.; McCamey, D. R.; Stenzel, M. H. Polydopamine as a visible-light photosensitiser for photoinitiated polymerisation. *Angew. Chem. Int. Ed.* **2023**, *62* (20), No. e202301678.
(35) Kim, J. H.; Lee, M.; Park, C. B. Polydopamine as a biomimetic electron gate for artificial photosynthesis. *Angew. Chem. Int. Ed.* **2014**, *53*, 6364−6368.
(36) Liu, S.-R.; Cai, L.-F.; Wang, L.-Y.; Yi, X.-F.; Peng, Y.-J.; He, N.; Wu, X.; Wang, Y.-P. Polydopamine coating on individual cells for enhanced extracellular electron transfer. *Chem. Commun.* **2019**, *55*, 10535−10538.
(37) Reggente, M.; Roullier, C.; Mouhib, M.; Brandl, P.; Wang, H.; Tacconi, S.; Mura, F.; Dini, L.; Labarile, R.; Trotta, M.; Fischer, F.; Boghossian, A. A. Polydopamine-coated photoautotrophic bacteria for improving extracellular electron transfer in living photovoltaics. *Nano Res.* **2024**, *17* (2), 866−874.
(38) Ryu, J. H.; Messersmith, P. B.; Lee, H. Polydopamine surface chemistry: A decade of discovery. *ACS Appl. Mater. Interfaces* **2018**, *10* (9), 7523−7540.
(39) Saiz-Poseu, J.; Mancebo-Aracil, J.; Nador, F.; Busqué, F.; Ruiz-Molina, D. The chemistry behind catechol-based adhesion. *Angew. Chem. Int. Ed.* **2019**, *58* (3), 696−714.
(40) Randviir, E. P. A Cross examination of electron transfer rate constants for carbon screen-printed electrodes using electrochemical impedance spectroscopy and cyclic voltammetry. *Electrochim. Acta* **2018**, *286*, 179−186.
(41) Takahashi, T. Routine management of microalgae using autofluorescence from chlorophyll. *Molecules* **2019**, *24* (24), 4441.
(42) Shi, Y.; Sun, M.; Zhang, Y.; Cui, J.; Wang, Y.; Shu, X.; Qin, Y.; Tan, H. H.; Liu, J.; Wu, Y. Structure modulated amorphous/crystalline WO_3 nanoporous arrays with superior electrochromic energy storage performance. *Sol. Energy Mater. Sol. Cells* **2020**, *212*, 110579.
(43) Martins, A. S.; Guaraldo, T. T.; Wenk, J.; Mattia, D.; Zanoni, M. V. B. Nanoporous WO_3 grown on a 3D tungsten mesh by electrochemical anodization for enhanced photoelectrocatalytic degradation of tetracycline in a continuous flow reactor. *J. Electroanal. Chem.* **2022**, *920*, 116617.
(44) Wey, L. T.; Bombelli, P.; Chen, X.; Lawrence, J. M.; Rabideau, C. M.; Rowden, S. J. L.; Zhang, J. Z.; Howe, C. J. The development of biophotovoltaic systems for power generation and biological analysis. *ChemElectroChem.* **2019**, *6* (21), 5375−5386.
(45) Souza, B. C. A.; Guaraldo, T. T.; Brugnera, M. F.; Pires, R. H.; Giannini, M. J. S. M.; Zanoni, M. V. B. Antifungal properties of high efficient W/WO_3 electrodes acting under UV-Vis and visible light and chloride medium. *J. Braz. Chem. Soc.* **2017**, *28*, 2084−2093.
(46) Feng, X.; Chen, Y.; Qin, Z.; Wang, M.; Guo, L. Facile fabrication of sandwich structured WO_3 nanoplate arrays for efficient

https://doi.org/10.1021/acselectrochem.5c00053
ACS Electrochem. 2025, 1, 1184−1193

photoelectrochemical water splitting. *ACS Appl. Mater. Interfaces* **2016**, *8* (28), 18089−18096.
(47) Szczesny, J.; Ruff, A.; Oliveira, A. R.; Pita, M.; Pereira, I. A. C.; De Lacey, A. L.; Schuhmann, W. Electroenzymatic CO_2 fixation using redox polymer/enzyme-modified gas diffusion electrodes. *ACS Energy Lett.* **2020**, *5*, 321−327.
(48) Alvarez-Malmagro, J.; Oliveira, A. R.; Gutiérrez-Sánchez, C.; Villajos, B.; Pereira, I. A. C.; Vélez, M.; Pita, M.; De Lacey, A. L. Bioelectrocatalytic activity of W-formate dehydrogenase covalently immobilized on functionalized gold and graphite electrodes. *ACS Appl. Mater. Interfaces* **2021**, *13* (10), 11891−11900.
(49) Fera, M.-C.; Manuel, R. R.; Pereira, I. A. C.; Abad, J. M.; De Lacey, A. L.; Pita, M. Carbon nanotubes - PEI - formate dehydrogenase nano-biointerface for the specific bioelectrochemical reduction of CO_2 to formate. *Carbon* **2023**, *209*, 118013.
(50) Cobb, S. J.; Dharani, A. M.; Oliveira, A. R.; Pereira, I. A. C.; Reisner, E. Carboxysome-inspired electrocatalysis using enzymes for the reduction of CO_2 at low concentrations. *Angew. Chem. Int. Ed.* **2023**, *62*, No. e202218782.
(51) Oliveira, A. R.; Mota, C.; Vilela-Alves, G.; Manuel, R. R.; Pedrosa, N.; Fourmond, V.; Klymanska, K.; Léger, C.; Guigliarelli, B.; Romão, M. J.; Cardoso Pereira, I. A. An allosteric redox switch involved in oxygen protection in a CO_2 reductase. *Nat. Chem. Biol.* **2024**, *20* (1), 111−119.

https://doi.org/10.1021/acselectrochem.5c00053
ACS Electrochem. 2025, 1, 1184−1193